

Performance comparison of a bridge-less canonical switching cell and H-bridge inverter with SVPWM fed PMLDLC motor drive under fuzzy logic controller

Jino Joy*, S. Ushakumari

Department of Electrical Engineering, Kerala University, College of Engineering Trivandrum 695 016, India

Corresponding Author Email: jinojoy8@gmail.com

https://doi.org/10.18280/mmc_a.910405

Received: 20 May 2018

Accepted: 15 September 2018

Keywords:

bridge-less canonical switching cell, H-bridge inverter, SVPWM, PMLDLC motor drive, fuzzy logic controller, speed control, torque ripple minimization, power factor correction

ABSTRACT

In this paper, speed control, torque ripple minimization and power factor correction of a bridge-less canonical switching cell and H-bridge inverter with space vector PWM fed permanent magnet brushless DC motor drive system with varying load is discussed. The constant speed of operation with minimum torque ripples and unity power factor operation during transient state is the most difficult control part in the motor drive system. At the starting condition, the current is too high due to the absence of back EMF and therefore the motor will start with high torque ripples. In order to eliminate these torque ripples during starting condition by limiting the starting current of the motor, it is necessary to have properly designed bridge-less canonical switching cell converter, H-bridge inverter and the intelligent controller, which will improve the power factor of the AC supply system and reliability of the PMLDLC motor drive. The performance parameters of a PMLDLC motor drive with this inverter and controller are analyzed through MATLAB/ Simulink and the real-time implementation is validated with 42BLF01 PMLDLC motor drive system

1. INTRODUCTION

Permanent Magnet Brushless DC (PMLDLC) motors make a challenging environment with brushed DC motors; because of their high efficiency, flux density per unit volume, low electromagnetic interference and wide range of speed control. Hence PMLDLC motors are chosen for many low and medium power applications such as aerospace, electric traction, robotics, ventilation, air conditioning etc.

The BLDC motor is a three-phase synchronous motor with stator having three-phase concentrated windings and the rotor having permanent magnets. The BLDC motor is also referred as an electronically commutated motor will work with a three-phase supply which is generated by an inverter unit. For controlling the three-phase inverter bridge, rotor position signals from the Hall Effect sensor [1] is utilized to determine the phase commutation in an inverter unit.

A front-end Bridge-less Canonical Switching Cell (BL-CSC) [2] not only controlled the DC link voltage but also make the inverter to operate at the low frequency so that switching losses are minimized and Unity Power Factor (UPF) is achieved at AC mains. Since the BL-CSC converter operation [3] is just similar to a battery source, which stores DC link voltage for the motor drive from an AC power source and provides complete isolation of PMLDLC motor drive system from an AC source. So the phase angle difference in voltage and current is approximately zero. Therefore, the BL-CSC converter fed PMLDLC motor drive provides nearly unity power factor operation even at varying load conditions. Main objective of the BL-CSC converter design in PMLDLC motor drive system is for improving the power factor at AC mains and to reduce the switching ripples [4] since the current does not change abruptly. Compared to the conventional CSC converter, the Bridge-less CSC converter provides improved

power factor in a PMLDLC motor drive even at varying load conditions since the absence of Diode Bridge Rectifier (DBR) circuit. The BL-CSC converter has the benefits of high input and low output impedance with large energy storage capacity when compared with other non-isolated converters.

For controlling the three-phase voltage supply generated in an inverter unit, proper commutation of each phase with space vector pulse width modulation [5] technique is employed. The SVPWM refers to a special switching sequence of a three-phase H-Bridge Inverter (H-BI) used in a PMLDLC motor drive system. The conventional voltage source inverter having three legs with six switching devices for the generation of three-phase voltage by proper commutation of each MOSFET switches in two legs. But, the H-bridge inverter having six legs with twelve switching devices for the generation of three-phase voltage by proper commutation of each MOSFET switches in four legs. The number of switching devices in H-bridge inverter is higher than conventional voltage source inverter, so it provides high current operation with minimum switching ripples in the source current. Therefore the H-Bridge inverter fed PMLDLC motor is preferred for high starting and running torque operations [6]. The H-bridge inverter with Space Vector PWM produces better torque ripple elimination in varying load conditions. The SVPWM method is an advanced computation intensive PWM method and possibly the best technique for variable frequency drive applications. The SVPWM technique utilizes DC bus voltage by 15% more than Sinusoidal PWM (SPWM) and generates less harmonic distortion [7] in three-phase inverters. The SVPWM technique provides an improved commutation of electronic switches from one phase to another phase [8] and thereby the current pulsations in source current and torque ripples in a PMLDLC motor drive are eliminated.

In this work, PMLDLC motor drive with fuzzy logic

controller is proposed for maintaining the rated speed of the motor under varying load conditions. The fuzzy logic controller, having two inputs and single output signals. The error (e) and change error (Δe) are the two input signals of fuzzy logic controller [9] and the single output signal is the duty cycle of PWM signal, used for the gate triggering of BL-CSC converter.

One of the main drawbacks associated with a BLDC motor is torque ripples [10]. Extensive research is progressing on the torque ripple reduction in BLDC motor with ideal trapezoidal back EMF. Generally, phase currents in a BLDC motor are controlled to follow a rectangular waveform which is considered to be ideal for the two-phase conducting mode of the BLDC motor [11]. During commutation, one phase is turned off and another phase is turned on. The mismatch between the decrease and increase slopes of these two-phase currents causes the current pulsation in the third phase which is turned on condition and results in torque ripples [12-18]. The torque ripples cause the mechanical vibration, acoustic noise and bearing damage and hence, reduce the life of the motor. Information on the accurate rotor position and back EMF is required to reduce the torque ripples of the motor with non-ideal trapezoidal back EMF [19].

The main objective of this work is the speed control, torque ripple minimization and power factor correction of a PMBLDC motor drive system during starting and varying load conditions. The principle of operation of H-bridge inverter fed PMBLDC motor drive is explained in section 2. Section 3 explains the design and operation of a BL-CSC converter. The SVPWM operation in a PMBLDC Motor is explained in section 4. The design of fuzzy logic controller is discussed in section 5. The simulation results of PMBLDC motor with varying load is analyzed using MATLAB/ Simulink software and explained in section 6. The hardware simulations using Proteus 8.0 software and experimental setup for proposed drive are discussed in sections 7-10. The conclusions and future scope of the work are explained in section 11.

2. PRINCIPLE OF OPERATION OF H-BRIDGE INVERTER FED PMBLDC MOTOR

The H-bridge inverter is multilevel inverter [20] can develop any number of levels of inverter output voltage. In this work, single level H-bridge inverter is proposed. At a time 2-MOSFET switches are turned ON for forwarding or reversing the stator current in a PMBLDC drive. For each phase is controlled by 4-MOSFET switches, that structure is similar to an H-bridge is shown in Figure 1.

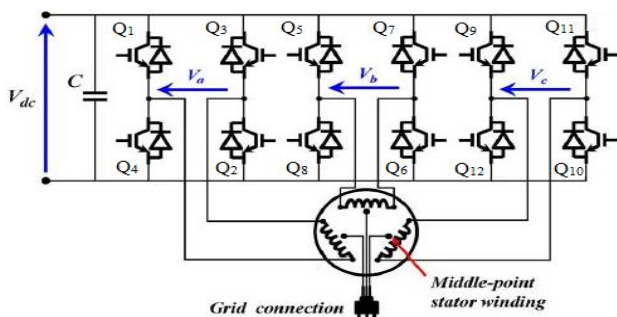


Figure 1. PMBLDC motor drive with H-bridge inverter

The H-bridge inverter having high current rating than

voltage source inverter since the number of driving MOSFET switches are high. Therefore the H-bridge inverter fed PMBLDC motor is preferred for high torque applications. The MOSFET switching is based on the rotor position of the PMBLDC motor drive and its hall sensor (H_a , H_b and H_c) signals [21-22]. The switching pattern in an H-bridge inverter based on the rotor position is shown in table 1.

Table 1. Clockwise hall sensor signals and drive signals

| Rotor Position | Hall Sensor Signals | | | Q ₁ | Q ₃ | Q ₅ | Q ₇ | Q ₉ | Q ₁₁ |
|----------------|---------------------|----------------|----------------|----------------|----------------|----------------|----------------|-----------------|-----------------|
| | H _a | H _b | H _c | Q ₂ | Q ₄ | Q ₆ | Q ₈ | Q ₁₀ | Q ₁₂ |
| | | | | | | | | | |
| NA | 0 | 0 | 0 | 0 | 0 | 0 | 0 | 0 | 0 |
| 0° – 60° | 1 | 0 | 0 | 1 | 0 | 0 | 0 | 0 | 1 |
| 60° – 120° | 1 | 1 | 0 | 0 | 0 | 1 | 0 | 0 | 1 |
| 120° – 180° | 0 | 1 | 0 | 0 | 1 | 1 | 0 | 0 | 0 |
| 180° – 240° | 0 | 1 | 1 | 0 | 1 | 0 | 0 | 1 | 0 |
| 240° – 300° | 0 | 0 | 1 | 0 | 0 | 0 | 1 | 1 | 0 |
| 300° – 360° | 0 | 0 | 1 | 1 | 0 | 0 | 1 | 0 | 0 |
| NA | 1 | 1 | 1 | 0 | 0 | 0 | 0 | 0 | 0 |

3. PRINCIPLE OF OPERATION OF BL-CSC CONVERTER

An uncontrolled single phase diode bridge rectifier feeding a BLDC motor via VSI injects a high amount of harmonics in the AC mains which are not recommended by International PQ (Power Quality) standards are given in IEC 61000-3-2. This paper presents a BLDC motor drive using a BL-CSC converter as a front end converter for PFC and improved power quality as shown in Figure 2. PFC is achieved by the discontinuous inductor current mode operation of the BL-CSC converter using a voltage follower approach, which requires sensing of dc-link voltage for voltage control and inherent PFC is achieved at AC mains [23]. The switch of front end BL-CSC converter is operated in high switching frequency for effective control and small size of devices like inductor; hence a high-frequency MOSFET of the suitable rating is used.

A reference voltage corresponding to the desired speed is obtained by multiplying the reference speed with voltage constant (K_b) of a BLDC motor. This reference voltage is compared with the sensed voltage of the DC link capacitor and produces an error voltage. The error voltage is given to the controller. Finally, a PWM signal is generated by comparing the controller output with a saw-tooth wave of high frequency which is given to the MOSFET's of the CSC converter for voltage control in DC bus.

The converter is operated in three different modes in every switching period [24], these are:

Mode I: In this mode, BL-CSC converter switch is ON, inductor charges the input current and capacitor C_1 , C_2 discharges the energy to the DC link capacitor C_d , the DC link capacitor is charging as well as supplies energy to the BLDC drive.

Mode II: In this mode, the BL-CSC converter switch is OFF, then the inductor L_1 , L_2 discharges the stored energy to the DC link capacitor through diode D_1 and D_2 . Now, the capacitor C_1 and C_2 charges the DC link voltage from the mains.

Mode III: This mode starts when the inductor current is

going to be zero, automatically a diode D_1 and D_2 goes into the reverse biased conditions, the capacitor C_1 and C_2 continues to

charging, then the DC link capacitor C_d discharges the energy to the VSI or H-BI fed BLDC motor drive.

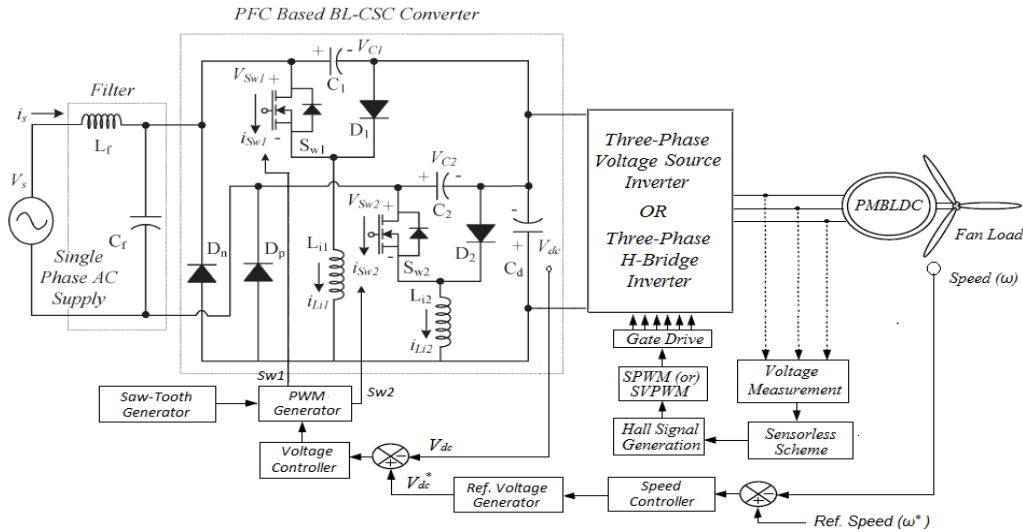


Figure 2. BL-CSC converter fed sensorless PMSBLDC drive

4. SPACE VECTOR PULSE WIDTH MODULATION IN A BLDC DRIVE

Space Vector Modulation is one of the preferred real time modulation techniques and is widely used for digital control of three-phase inverters [26]. The principle and implementation of the space vector modulation for the two-level inverter [27] is presented in this section. A 3-phase BLDC motor can be controlled by creating a rotating voltage reference vector within a hexagon; the speed of rotation of this voltage reference vector determines the frequency of motor rotation [28]. It can be shown that SVPWM can directly transform the stator voltage vectors from α - β co-ordinate system to PWM signals [29]. Space vector pulse width modulation is one of the most efficient methods for this purpose which relies on analysis of three-phase inverter in the complex plane by the space vector theory [30]. SVPWM controls the motor based on the switching of the space voltage vectors by which an approximate circular rotary magnetic field is obtained. Six switching states are generated according to the position of the rotor by using position signal feedback given by three Hall Effect sensors.

Consider the three-phase voltages V_a , V_b and V_c are generated from an inverter unit which is displaced by 120° ,

$$\begin{aligned} V_a &= V_m \sin(\omega t) \\ V_b &= V_m \sin(\omega t - 120^\circ) \\ V_c &= V_m \sin(\omega t + 120^\circ) \end{aligned}$$

Where, V_m is the maximum value of an inverter output voltage. These three vectors can be represented by one vector which is known as space vector. Consider V_s , which is a vector having magnitude of $0.667V_m$ and rotates in space at ω rad/s as shown in Figure 3,

$$\begin{aligned} V_s &= \frac{2}{3} [V_a + V_b e^{j\frac{2\pi}{3}} + V_c e^{-j\frac{2\pi}{3}}] \\ V_s &= \frac{2}{3} V_m [\sin(\omega t) - j \cos(\omega t)] \end{aligned}$$

This vector can be represented in two-dimensional space [31] by simply resolving abc into d-q axis as shown in Figure 4.

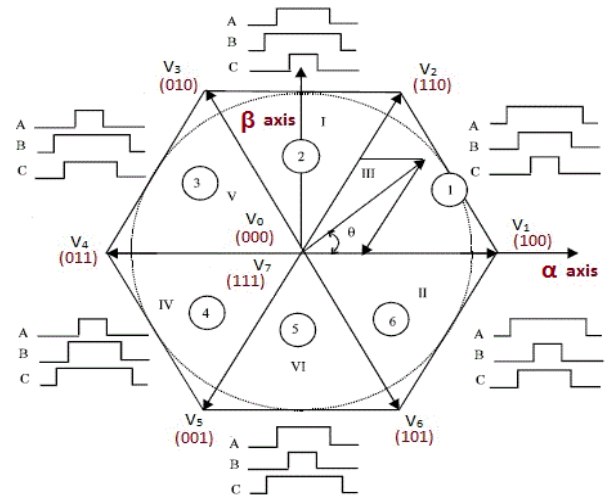


Figure 3. Basic switching vectors and sectors

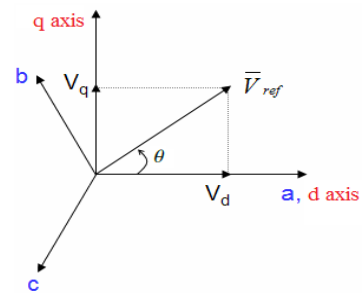


Figure 4. Voltage space vector components in d-q axis

The space vector voltage components V_d , V_q , V_{ref} and phase angle (θ) can be determined as:

$$\begin{aligned} V_d &= V_{an} - V_{bn} \cos 60^\circ - V_{cn} \cos 60^\circ = V_{an} - \frac{V_{bn}}{2} - \frac{V_{cn}}{2} \\ V_q &= V_{an} \times 0 + V_{bn} \sin 60^\circ - V_{cn} \sin 60^\circ \\ &= \frac{\sqrt{3}}{2} V_{bn} - \frac{\sqrt{3}}{2} V_{cn} \end{aligned}$$

Therefore the space vector can be written as,

$$\begin{bmatrix} V_d \\ V_q \end{bmatrix} = \frac{2}{3} \begin{bmatrix} 1 & -\frac{1}{2} & -\frac{1}{2} \\ 0 & \frac{\sqrt{3}}{2} & -\frac{\sqrt{3}}{2} \end{bmatrix} \begin{bmatrix} V_a \\ V_b \\ V_c \end{bmatrix}$$

$$|V_{ref}| = V_d + jV_q$$

$$\theta = \tan^{-1} \left(\frac{V_q}{V_d} \right)$$

The transformation from the d-q axis to the $\alpha - \beta$ axis is found by Clarks transformation [32], which is rotating with an angular velocity of ω rad/s, can be obtained by rotating the d-q axis with ωt and is given by

$$\begin{bmatrix} V_\alpha \\ V_\beta \end{bmatrix} = \begin{bmatrix} \cos(\omega t) & \cos(\omega t + \frac{\pi}{2}) \\ \sin(\omega t) & \sin(\omega t + \frac{\pi}{2}) \end{bmatrix} \begin{bmatrix} V_d \\ V_q \end{bmatrix} = \begin{bmatrix} \cos(\omega t) & -\sin(\omega t) \\ \sin(\omega t) & \cos(\omega t) \end{bmatrix} \begin{bmatrix} V_d \\ V_q \end{bmatrix}$$

The three-phase bridge voltage source inverter with eight possible switching states is shown in Figure 5. The typical diagram of a three-phase voltage source inverter model having six power MOSFET switches S_1 to S_6 that shape the output voltage, which are controlled by the switching variables a, a', b, b', c and c'.

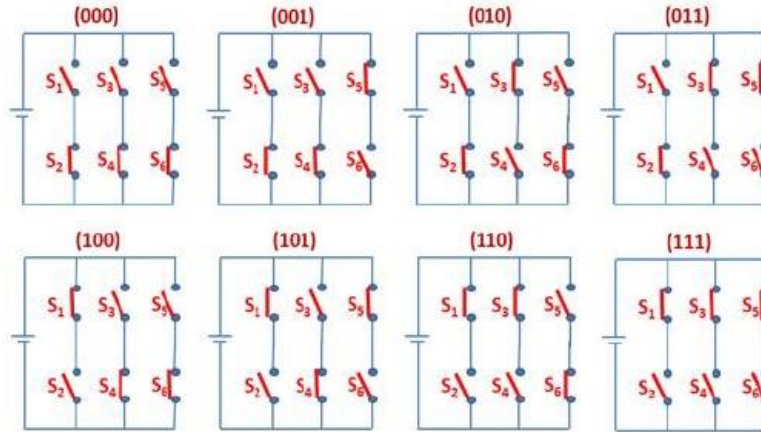


Figure 5. Possible switching combinations in six step control

When an upper MOSFET is switched ON, i.e., when a, b or c is 1, the corresponding lower MOSFET is switched OFF, i.e., the corresponding a', b' or c' is 0. When upper switch is ON, the potential of a, b and c is $0.5 V_{dc}$. When lower switch is ON, the potential of a, b and c is $-0.5 V_{dc}$. Therefore, the ON and OFF states of the upper MOSFET's S_1 , S_3 and S_5 can be used to determine the output voltage. Hence there are eight possible switch states, i.e., (0,0,0), (0,0,1), (0,1,0), (0,1,1), (1,0,0), (1,0,1), (1,1,0), (1,1,1). The inverter has six states when a voltage is applied to the motor and two states when the motor is shorted through the upper or lower MOSFET's resulting in zero volts being applied to the motor.

The magnitude and phase angle of space vector for all possible switching states are,

- For (0, 0, 0): $V_s = 0 < 0^\circ - V_0$
- For (1, 0, 0): $V_s = V_{dc} < 0^\circ - V_1$
- For (1, 1, 0): $V_s = V_{dc} < 60^\circ - V_2$
- For (0, 1, 0): $V_s = V_{dc} < 120^\circ - V_3$
- For (0, 1, 1): $V_s = V_{dc} < 180^\circ - V_4$
- For (0, 0, 1): $V_s = V_{dc} < 240^\circ - V_5$
- For (1, 0, 1): $V_s = V_{dc} < 300^\circ - V_6$
- For (1, 1, 1): $V_s = 0 < 0^\circ - V_7$

There are six non-zero vectors (V_1 to V_6) and two zero vectors (V_0 and V_7). Table 2 summarizes switching vectors along with the corresponding line to neutral voltages and line to line voltages applied to the motor.

Table 2. Switching patterns and output vectors

| Voltage Vectors | Switching Vectors | | | Line to Neutral Voltage | | | Line to Line Voltage | | |
|-----------------|-------------------|---|---|-------------------------|----------|----------|----------------------|----------|----------|
| | A | B | C | V_{an} | V_{bn} | V_{cn} | V_{ab} | V_{bc} | V_{ca} |
| V_0 | 0 | 0 | 0 | 0 | 0 | 0 | 0 | 0 | 0 |
| V_1 | 1 | 0 | 0 | $2/3$ | $-1/3$ | $-1/3$ | 1 | 0 | -1 |
| V_2 | 1 | 1 | 0 | $1/3$ | $1/3$ | $-2/3$ | 0 | 1 | -1 |
| V_3 | 0 | 1 | 0 | $-1/3$ | $2/3$ | $-1/3$ | -1 | 1 | 0 |
| V_4 | 0 | 1 | 1 | $-2/3$ | $1/3$ | $1/3$ | -1 | 0 | 1 |
| V_5 | 0 | 0 | 1 | $-1/3$ | $1/3$ | $2/3$ | 0 | -1 | 1 |
| V_6 | 1 | 0 | 1 | $1/3$ | $-2/3$ | $1/3$ | 1 | -1 | 0 |
| V_7 | 1 | 1 | 1 | 0 | 0 | 0 | 0 | 0 | 0 |

5. THEORETICAL DESIGN OF FUZZY LOGIC CONTROLLERS

Fuzzy Logic Controllers (FLC) do not require an exact mathematical model, they are designed based on general knowledge of the plant [35]. Fuzzy logic control is a control algorithm based on a linguistic control strategy which tries to

account the humans knowledge about how to control a system without requiring a mathematical model. Figure 10 shows the basic structure of a fuzzy logic controller for PMBLDC motor drive.

FLC is used to improve the dynamic response [36] and reduce the overshoot before the motor reaches the desired speed. Inputs of FLC are speed error and the differential of

speed error. Output of the controller is PWM duty cycle.

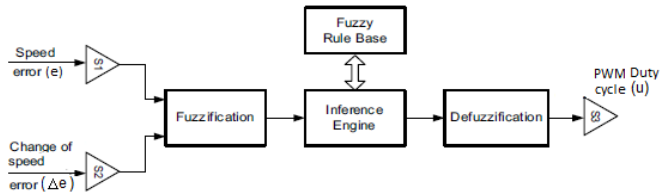


Figure 6. General structure of fuzzy logic controller

The fuzzy logic controller is composed of four elements; fuzzification, fuzzy rule base, fuzzy inference engine and defuzzification. The design steps are as follows.

(i) Fuzzification: Fuzzy logic uses linguistic variables instead of numerical variables. The process of converting a numerical variable into a linguistic variable is called fuzzification. To perform fuzzy logic computation, the inputs must be converted from numerical or crisp value into fuzzy values and the output should be converted from fuzzy value to crisp value.

Design of fuzzy logic controllers [37] adapt the varying operating points. The fuzzy logic variables i.e., error (e), change in error (Δe) and change in duty-cycle (u) are quantified using the following linguistic terms: Negative Big (NB), Negative Medium (NM), Negative Small (NS), Zero (Z), Positive Small (PS), Positive Medium (PM) and Positive Big (PB). Fuzzy logic membership functions are used as tools to convert crisp values to linguistic terms [38]. A fuzzy variable can contain several fuzzy subsets within, depending on how many linguistic terms are used. Each fuzzy subset represents one linguistic term. In order to define a fuzzy logic membership function, the designer can choose many different shapes such as triangle, a trapezoid, a Bell shaped based on their preference and experience. In this work, triangular and trapezoidal membership functions are used for the real-time implementations due to their simple formulas and computational efficiency.

(ii) Fuzzy Logic Rule Base: Instead of using mathematical formula, FLC uses fuzzy logic rules to make a decision and generate the control action. The rules are in the form of IF-THEN statements. The fuzzy inference operation is implemented by using forty-nine fuzzy logic rules, which is given in Figure 7.

| | | Error | | | | | | |
|--------------|----|-------|----|----|----|----|----|----|
| | | NB | NM | NS | ZO | PS | PM | PB |
| Change Error | NB | NB | NB | NB | NB | NM | NS | ZO |
| | NM | NB | NB | NB | NM | NS | ZO | PS |
| | NS | NB | NB | NM | NS | ZO | PS | PM |
| | ZO | NB | NM | NS | ZO | PS | PM | PB |
| | PS | NM | NS | ZO | PS | PM | PB | PB |
| | PM | NS | ZO | PS | PM | PB | PB | PB |
| | PB | ZO | PS | PM | PB | PB | PB | PB |

Figure 7. Fuzzy logic rules

1. If error is NB and change in error is NB then output is NB.
 2. If error is NB and change in error is PS then output is NM.
 3. If error is NB and change in error is PB then output is ZO.
- (iii) Defuzzification: The fuzzy logic controller output is

converted into real value output i.e. crisp output by the process called defuzzification. Even though many defuzzification methods are available [39], the most preferred one is a centroid method because it can be easily implemented and requires less computation time when implemented in digital control systems. The formula for this method is given by,

$$Z = \frac{\sum_{x=1}^n \mu(x) \times x}{\sum_{x=1}^n \mu(x)}$$

Where Z is the defuzzified value, $\mu(x)$ is the membership value of member x. This crisp value which is either positive or negative is added to the previous output to control the duty-cycle of the switching devices in the power inverter so as to maintain the rated speed of the PMSBLDC motor drive by controlling the applied voltage across the stator winding.

6. SIMULATION RESULTS

6.1 BLDC motor with fuzzy logic controller

Figure 8 shows an inverter output voltage across the phases A, B and C. The trapezoidal shape line voltage is generated from the three-phase H-bridge inverter by proper commutation of MOSFET switches using SVPWM technique. The line voltage is attained its rated value as 24 V when the motor attains the rated speed. If the motor under the varying load condition, the line voltage changes from 24 V to 30 V by varying the DC link voltage generated from the BL-CSC converter and makes the rotor speed constant.

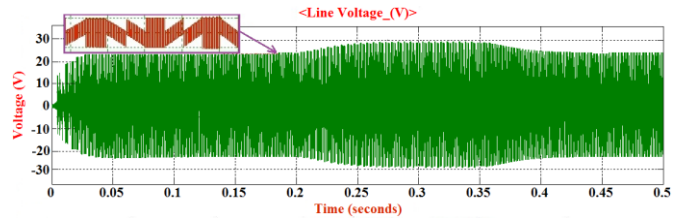


Figure 8. Inverter output voltage

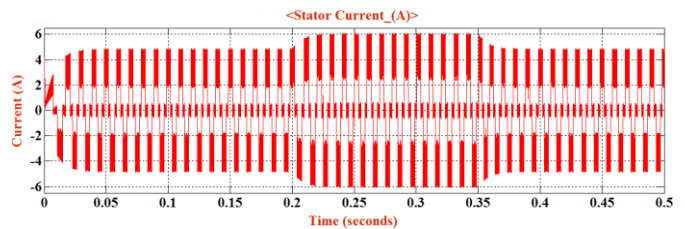


Figure 9. Stator current in each phase of BLDC motor drive

Figure 9 shows the stator currents in a BLDC motor with a fuzzy logic controller having the rectangular shape and high starting current with less harmonics. The starting current and running current is 5 A which changes during transients for maintaining the stability of the motor speed.

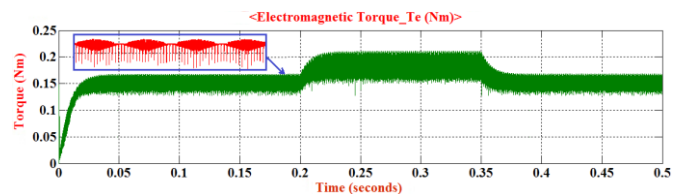


Figure 10. Electromagnetic torque in a PMSBLDC motor

Figure 10 shows the electromagnetic torque developed in a PMSBLDC motor with fuzzy logic controller. At starting, the input current and torque are high, since back EMF $E_b = 0$. So the motor is able to start with the load. The starting and running torques of the motor is 0.17 Nm. During transient state, the motor maintains the rated torque as 0.22 N m within 0.02 seconds after transients. Figure 11 shows rotor speed response in a PMSBLDC drive. The time required to attain the rated speed is 0.04 seconds. The increasing load is applied to 0.20 second and decreasing load is applied at 0.35 second. In both cases, it is seen that the motor attains the rated speed within 0.03 seconds.

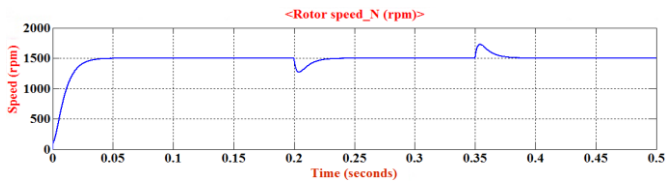


Figure 11. Speed response with fuzzy logic controller

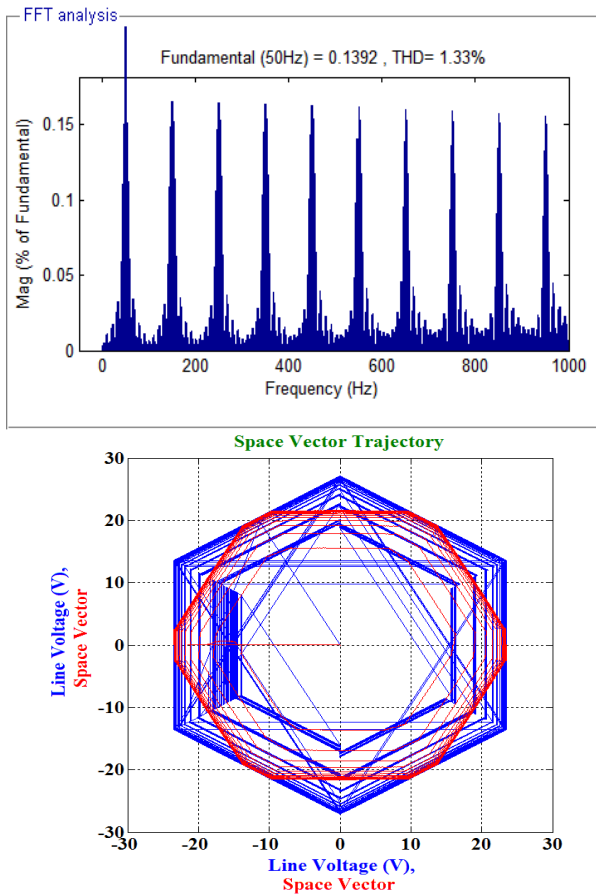


Figure 12. THD and space vector trajectory of the system with fuzzy logic controller

Figure 12 shows the Total Harmonic Distortion (THD) of supply current in SVPWM fed PMSBLDC motor drive with fuzzy logic controller during transient conditions.

$$\text{Power Factor, } pf = \frac{D.F}{\sqrt{1+THD^2}} = \frac{0.999}{\sqrt{1+0.0133^2}} = 0.9989.$$

The space vector trajectory generated with line voltage during the simulation of PMSBLDC motor drive with a fuzzy logic controller in MATLAB/ Simulink software. The space vector having a hexagonal shape and starts from center i.e.,

line voltage is zero and attain the complete diameter at rated voltage of 24 V.

7. EXPERIMENTAL SETUP FOR PROPOSED DRIVE

For the hardware implementation purpose, 42BLF01 BLDC motor is preferred which is shown in Figure 13. The motor specification details are explained in the table 3.

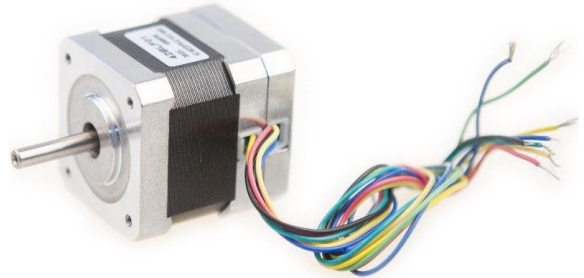


Figure 13. 42BLF01 BLDC motor

Table 5. Electrical specifications of 42BLF01 BLDC motor

| Model | 42BLF01 BLDC Motor |
|------------------------|--------------------|
| Number of poles | 8 |
| Number of phases | 3 |
| Rated voltage V_{DC} | 24 |
| Rated speed | 4000 rpm |
| Rated torque | 0.063 Nm |
| Rated current | 1.9 A |
| Output power | 26 W |
| Peak torque | 0.18 Nm |
| Peak current | 5.7 A |
| Body length | 47 mm |
| Mass | 0.29kg |

To control a three phase BLDC motor, three phase H-bridge inverters are used to switch the three phases ON and OFF. The H-bridge circuit consists of 6 N-channel and 6 P-channel MOSFET switches with other electronic components are used. For controlling the speed of BLDC motor through PWM operation in three-phase inverter switching by IC74LS08 AND gate and varying the motor speed by 10K potentiometer unit. Figure 14 shows the hardware implemented structure of three-phase H-bridge inverter circuit. The commutation of MOSFET's in the H-BI based on the rotor position signals from the Hall effect sensor.

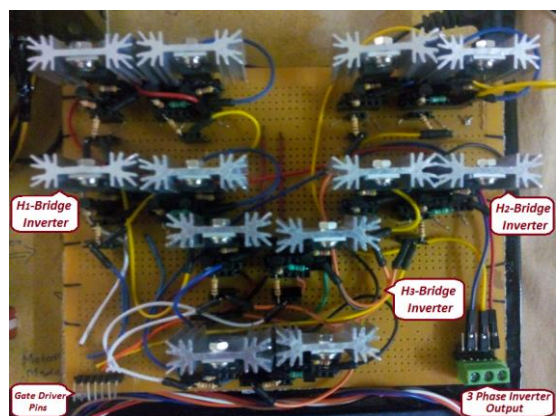


Figure 14. Three phase H-bridge inverter

8. EXPERIMENTAL SETUP FOR BL-CSC CONVERTER

The input voltage for BL-CSC converter from the transformer 230 V/ 24 V and the amplitude of voltage is 24 V which is shown in Figure 15. The voltage stored in the BL-CSC converter is in opposite polarity of supply voltage and its magnitude is -24 V as shown in Figure 16. The BL-CSC converter is just similar to a battery source by storing voltage from the mains and provide better isolation from the AC source. So the BL-CSC converter fed PMBLDC motor drive produce approximately UPF operation at AC mains.

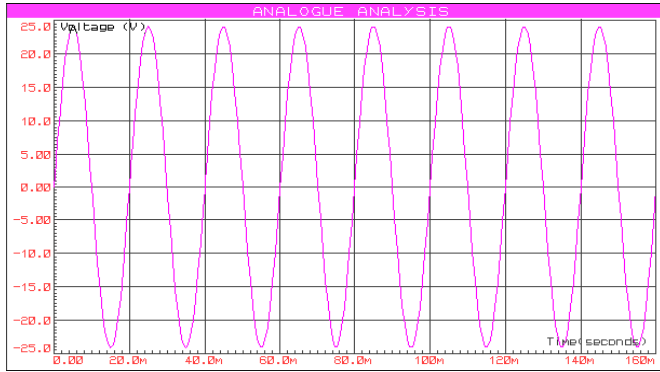


Figure 15. BL-CSC converter input voltage

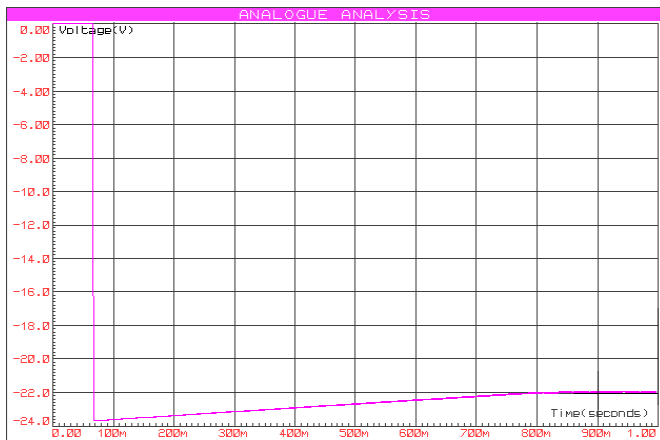


Figure 16. BL-CSC converter output voltage

9. EXPERIMENTAL RESULTS

The DC link voltage of 24 V is produced by a BL-CSC converter is fed to the three-phase H-bridge inverter. The DC link current and stator current of phases A, B and C of BL-CSC converter is shown in figs. 17 & 18. The DC-link starting current is 3.90 A and normal operating current is 1.90 A. Also, the starting phase current is 1.85 A and running current is 0.90 A. Figs. 19 & 20 shows the inverter output voltage and rotor speed response of PMBLDC motor. The amplitude of output voltage is 24 V and rectangular in shape. The set speed of the BLDC motor is 1500 rpm, it attains the speed of 1490 rpm.

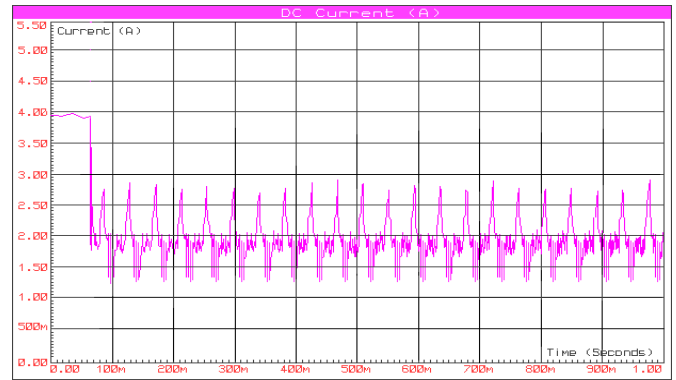


Figure 17. DC link current of BLDC motor

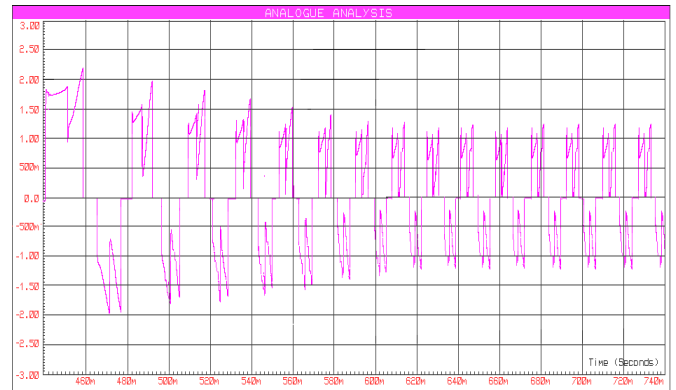


Figure 18. Stator current of BLDC motor

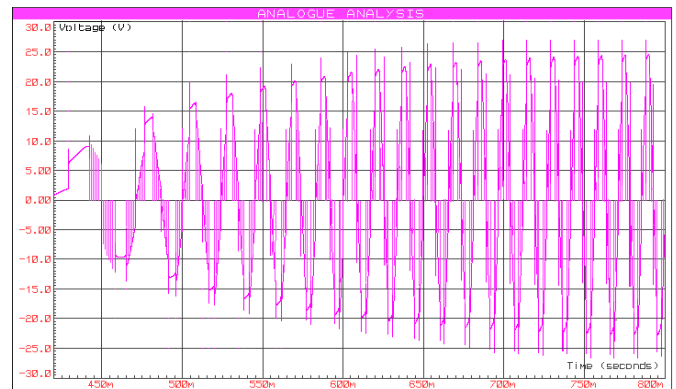


Figure 19. Inverter output voltage of BLDC motor

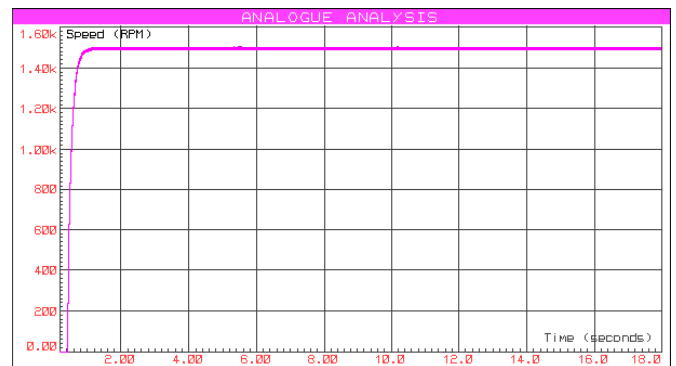


Figure 20. Rotor speed response of BLDC motor

10. CONCLUSION

In this paper, the performance comparison of a bridge-less canonical switching cell converter and H-BI with space vector PWM fed PMBLDC motor drive under fuzzy logic controller during varying a load is discussed. PMBLDC motor with fuzzy logic controller offers high starting torque with minimum torque ripple and approximately unity power factor. During transient conditions, fuzzy logic controlled BLDC motor with SVPWM overcomes the instability and maintain rated speed within 0.04 seconds. The simulation results are experimentally validated and implemented through the PIC16F877A and Arduino Mega 2560 controllers. This makes the PMBLDC motor drives suitable for the applications like electric traction, aerospace, robotics and industrial automation. In future, the Multi-level H-Bridge inverter can be proposed for reducing the current ripples in an inverter unit during commutation from one phase to another phase. Also, the regenerative braking mode of operation in a PMBLDC motor will improve the overall efficiency of the drive system.

REFERENCES

- [1] Baszynski M, Pirog S. (2014). A novel speed measurement method for a high-speed BLDC motor based on the signals from the rotor position sensor. *IEEE Trans. Ind. Electron* 10(1): 84-91. <https://doi.org/10.1109/TII.2013.2243740>
- [2] Williams BW. (2015). Generation and analysis of canonical switching cell DC to DC converters. *IEEE Trans. on Industrial Electronics* 61(1): 329 - 346. <https://doi.org/10.1109/TIE.2013.2240633>
- [3] Singh B, Bist V. (2015). A BL-CSC converter-fed BLDC Motor drive with power factor correction. *IEEE Trans. on Industrial Electronics* 62(1): 172-183. <https://doi.org/10.1109/TIE.2014.2327551>
- [4] Singh B, Bist V. (2014). Reduced sensor based improved power quality CSC converter fed BLDC motor drive. *IEEE International Conference on Power Electronics and Drives Systems*: 1-6. <https://doi.org/10.1109/PEDES.2012.6484280>
- [5] Li XS, Deng ZQ, Chen ZD, Fei QZ. (2011). Analysis and simplification of three- dimensional space vector PWM for three phase four leg inverters. *IEEE Trans. on Industrial Electronics* 58(2): 450-464. <https://doi.org/10.1109/TIE.2010.2046610>
- [6] Wang HZ. (2012). Design and implementation of brushless DC motor drive and control system. *Procedia Engineering. International Workshop on Information and Electronics Engineering (IWIEE)* 29: 2219-2224. <https://doi.org/10.1016/j.proeng.2012.01.291>
- [7] Viswanatha V, Jeevananthan S. (2013). A novel space-vector current control method for commutation torque ripple reduction of brushless DC motor drive. *AJSE*. 38(10): 1773-2784. <https://doi.org/10.1007/s13369-012-0490-0>
- [8] Grandi G, Loncarski J, Dordevic O. (2015). Analysis and comparison of peak-to-peak current ripple in two-level and multilevel PWM inverters. *IEEE Transactions on Industrial Electronics* 62(5): 2721-2730. <https://doi.org/10.1109/TIE.2014.2363624>
- [9] Siong TC, Ismail B, Isa ZM. (2010). Study of fuzzy and PI controller for permanent magnet brushless DC motor drive. The 4th International Power Engineering and Optimization Conference, Shah Alam, Selangor, Malaysia: 517-521. <https://doi.org/10.1109/PEOCO.2010.5559256>
- [10] Firdaus M, Ishak D, Hassan AHA. (2011). A comparative study of PI, fuzzy and hybrid PI fuzzy logic controller for speed control of brushless DC motor drive. *International conference on computer applications and industrial electronics*: 189-194. <https://doi.org/10.1109/ICCAIE.2011.6162129>
- [11] Yang F, Jiang CG, Allan Taylor, Hua Bai, Argun Yetkin and Arda Gundogan (2014). Design of a high efficiency minimum torque ripple 12 V/1 kW three phase BLDC motor drive system for diesel engine emission reductions. *IEEE Trans. Power Electron* 63(7): 3107-3114. <https://doi.org/10.1109/TVT.2014.2300931>
- [12] Xia CL, Shi TN, Chen W. (2017). A current control scheme of brushless DC motors driven by four-switch three-phase inverters. *IEEE Journal of Emerging and Selected Topics in Power Electronics* 5(1): 547-558. <https://doi.org/10.1109/JESTPE.2016.2637383>
- [13] Sheng TT, Wang XL, Zhang JL, Deng ZQ. (2014). Torque ripple mitigation for brushless DC machine drive systems using one-cycle average torque control. *IEEE Trans. Ind. Electron* 62(4): 2114-2122. <https://doi.org/10.1109/TIE.2014.2351377>
- [14] Sung J, HanW, Lee MH, Harashima F. (2010). A new approach for minimum torque ripple maximum efficiency control of BLDC motor. *IEEE Trans. Ind. Electron* 47(1): 109-114. <https://doi.org/10.1109/41.824132>
- [15] Liu Y, Zhu ZQ, Howe D. (2012). Direct torque control of brushless DC drives with reduced torque ripple. *IEEE Trans. Ind. Electron* 41(2): 599-608. <https://doi.org/10.1109/TIA.2005.844853>
- [16] Xu YX, Wei YY, Wang BC. (2015). A novel inverter topology for brushless DC motor drive to shorten commutation time. *IEEE Trans. on Ind. Electronics* 63(2): 796-807. <https://doi.org/10.1109/TIE.2015.2480759>
- [17] Li XM, Xia CL. (2016). Commutation torque ripple reduction strategy of Z-source inverter fed brushless DC motor. *IEEE Trans. on Power Electronics* 31(11): 7677-7690. <https://doi.org/10.1109/TPEL.2016.2550489>
- [18] Tan Y, Dong B, Bi C. (2016). Dynamic commutation torque-ripple reduction for brushless DC motor based on quasi-Z-source net. *IET Electronic Power Appl.* 10(9): 819-826. <https://doi.org/10.1049/iet-epa.2016.0219>
- [19] Shi TN, Cao YF, Jiang GK. (2017). A torque control strategy for torque ripple reduction of brushless DC motor with non-ideal back electromotive force. *IEEE Transactions on Industrial Electronics* 64(6): 4423-4433. <https://doi.org/10.1109/TIE.2017.2674587>
- [20] Ahmadi R, Ferdowsi M. (2012). Double-input converters based on H-bridge cells: Derivation, small-signal modeling and power sharing analysis. *IEEE Trans. on Circuits and Systems* 59(4): 875-888. <https://doi.org/10.1109/tcsi.2011.2169910>
- [21] Yang YP, Ting YY. (2014). Improved angular displacement estimation based on hall-effect sensors for driving a brushless permanent-magnet motor. *IEEE Trans. On Industrial Electronics* 61(1): 504-511. <https://doi.org/10.1109/TIE.2013.2247013>
- [22] Dong LH, Huang YW, Liu JL. (2016). Improved fault tolerant control for brushless permanent magnet motor

- drives with defective hall sensors. *IEEE Trans. On Energy Conversion* 31(2): 789-799. <https://doi.org/10.1109/TEC.2016.2526621>
- [23] Singh B, Bist V. (2015). A PFC based BLDC motor drive using a canonical switching cell converter. *IEEE Trans. on Industrial Informatics* 10(2): 1207-1215. <https://doi.org/10.1109/TII.2014.2305620>
- [24] Singh B, Anand A. (2016). A PFC based SRM motor drive using a canonical switching cell converter. *IEEE 6th International Conference on Power Systems (ICPS)*. <https://doi.org/10.1109/ICPES.2016.7584246>
- [25] Singh S, Bist V, Singh B. (2015). Power factor correction in switched mode power supply for computers using canonical switching cell converter. *IET Power Electron* 8(2): 234-244. <https://doi.org/10.1049/iet-pel.2014.0123>
- [26] Lakhimsetty S, Surulivel N, Somasekhar VT. (2017). Improved SVPWM Strategies for an Enhanced Performance for a Four-Level Open-End Winding Induction Motor Drive. *IEEE Transactions on Industrial Electronics* 64(4): 2750-2759. <https://doi.org/10.1109/TIE.2016.2632059>
- [27] Tripura P, Kishorebabu YS, Tagore YR. (2011). Space vector pulse width modulation schemes for two-level voltage source inverter. *ACEEE Int. J. on Control System and Instrumentation* 2(3).
- [28] Zeng ZY, Jin XL, Zhao RX. (2017). Hybrid space vector modulation strategy for torque ripple minimization in three-phase four-switch inverter-fed PMSM drives. *IEEE Transactions on Industrial Electronics* 64(3): 2122-2134. <https://doi.org/10.1109/TIE.2016.2625768>
- [29] Shi TN, Niu XZ. (2017). Commutation torque ripple reduction of brushless DC motor in braking operation. *IEEE Transactions on Power Electronics* 54(12): 2435-2448. <https://doi.org/10.1109/TPEL.2017.2675444>
- [30] An QT, Peng Z, Sun LZ. (2016). Dual-space vector control of open-end winding permanent magnet synchronous motor drive fed by dual inverter. *IEEE Trans. On Power Electronics* 31(12): 8329-8342. <https://doi.org/10.1109/TPEL.2016.2520999>
- [31] Sasi D, Jisha KP. (2013). Modelling and simulation of SVPWM inverter fed permanent magnet brushless DC motor drive. *International Journal of Advanced Research in Electrical, Electronics and Instrumentation Engineering* 2(5): 1947-1955.
- [32] Michael PA, Suresh Kumar S. (2010). Simulation and comparison of SPWM and SVPWM control for three phase inverter. *ARPN Journal of Engineering and Applied Sciences* 5(7): 61-74.
- [33] Li ZG, Gao XF, Wang JH. (2016). Phase back EMF space vector oriented control of brushless DC motor for torque ripple minimization. *IEEE International Power Electronics and Motion Control Conference*. <https://doi.org/10.1109/IPEMC.2016.7512702>
- [34] Jiang WD, Huang H, Wang L. (2017). Commutation analysis of brushless DC motor and reducing commutation torque ripple in the two-phase stationary frame. *IEEE Transactions on Power Electronics* 32(6): 4675-4682. <https://doi.org/10.1109/TPEL.2016.2604422>
- [35] Topalov A, Dimitrov N, Bonev E. (2016). Industrial implementation of a fuzzy logic controller for brushless DC motor drives using the picomotion control framework. *IEEE International Conference on Intelligent Systems*. <https://doi.org/10.1109/IS.2016.7737493>
- [36] Nag T, Chatterjee A, Santra SB. (2016). Fuzzy logic-based loss minimisation scheme for brushless DC motor drive system. *IET Power Electron* 9(8).
- [37] Yan WS, Lin H, Li H, Yan W. (2012). Sensorless direct torque controlled drive of brushless DC motor based on fuzzy logic. *IEEE Trans. on Ind. Elec. and Appl.* 23(4): 3411-3416. <https://doi.org/10.1109/ICIEA.2009.5138835>
- [38] Baharudin NN, Ayob SM. (2015). Brushless DC motor drive control using single input fuzzy PI controller (SIFPIC). *IEEE International Conference on Power and Energy (PECon)*: 13-18. <https://doi.org/10.1109/CENCON.2015.7409506>
- [39] Muhammed Zakariah K, Yadaiah N. (2010). Digital implementation of fuzzy logic controller for wide range speed control of brushless DC motor. *IEEE Trans. on Ind. Elec.* (9): 119-124. <https://doi.org/10.1109/ICVES.2009.5400189>